Calil Amaral

MECHANICAL PROPERTIES OF METALLIC COMPONENTS ADDITIVELY MANUFACTURED BY DIRECTED ENERGY DEPOSITION LASER WITH POWDER AS FEEDSTOCK MATERIAL

Master thesis Project presented to the Programa de Pós-Graduação em Engenharia Mecânica from the Universidade Federal de Santa Catarina as part of the requirements to obtain a master's degree in Mechanical Engineering.

Orientador: Prof. Dr. Eng. Milton Pereira

Coorientador: Prof. Dr.-Ing. Walter Lindolfo Weingartner

Área de concentração: Fabricação.

Florianópolis

2019

SUMÁRIO

1 INTRODUCTION 3

1.1 GOALS 5

1.1.1 General goals 5

1.1.2 Specific goals 5

2 LIRETATURE REVIEW 6

2.1 ADDITIVE MANUFACTURING 6

2.1.1 Directed Energy Deposition 7

2.1.2 Laser technology 8

2.2 DIRECTED ENERGY DEPOSITION LASER WITH POWDER (DED-LP) ... 9

2.2.1 Process description 11

2.2.2 Thermal cycles and reported effects 13

2.2.3 Residual porosity and reported effects 14

2.2.4 Reported strength and dependence on other factors 15

3 MATERIALS AND METHODS 16

3.1 METHODOLOGY 16

3.2 TECHNICAL AND FINANCIAL RESOURCES 17

2. SCHEDULE 18

4 REFERENCES 19

1 INTRODUCTION

Additive manufacturing (AM) has gained attention for the last two decades for its great potential to reduce the time between ideation and production of complex geometries. This characteristic is being frequently explored among researchers and engineers to evaluate and compare product concepts beyond virtual models and prior to investing in tooling for mass production. The reduced supply chain, also has an enormous potential to decrease the lead time between a sales order and the delivery of a functional component, consequently reducing inventory cost [1].

Another great potential of the technology is the reduction of geometric constraints, removing barriers to the production of components optimized for multi-physics restrictions. Such optimizations can result in lower assembly part count and component weight, leading to more efficient operation and less fuel consumption in systems such as airplanes [2][3]. Figure 1 illustrates applications of different AM technologies used in the aerospace industry.

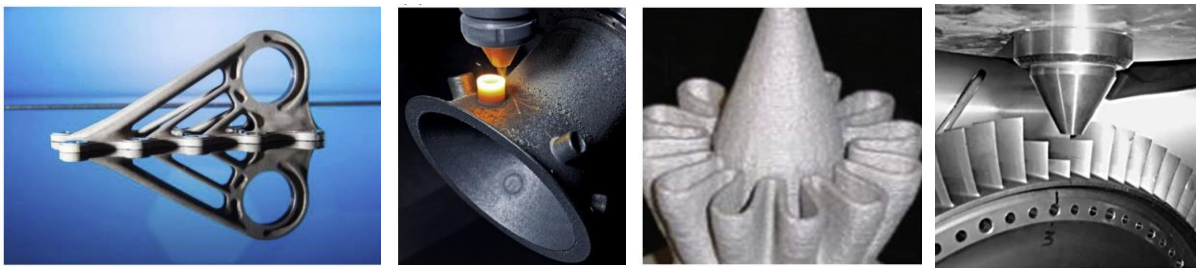

(a) (b) (c) (d)

Figure 1 - Examples of additive manufacturing of metallic components. (a) LBM-produced Ti-6Al-4V bracket for Airbus A350 with topology optimized bionic design resulting in ~30% weight saving cp. to conventional milled bracket [3][4] *; (b) Turbine housing fabricated by the LASERTEC 65 3D System using multi-axis deposition; (c) Exhaust duct fabricated using the Laser Engineered Net Shape (LENS) process* [3]*;(d) Repairing for damaged titanium blisk* [5].

Despite the promising features AM is still expensive when compared to other manufacturing processes, especially for processing metals, with only a few technologies applicable to manufacture dense components. To accomplish that, Powder Bed Fusion (PBF), Sheet Lamination (SL) and Directed Energy Deposition (DED) are some of the AM groups of process available, each one presenting particular strengths and limitations [1].

Among the above mentioned categories, Directed Energy Deposition Laser with Powder as feedstock material (DED-LP), a sub category of DED processes, offers advantages such as suitability to repair failed components, suitability to produce larger parts with higher build rates

when compared to PBF technology [16] and the potential to manufacture components with variations in alloy composition along the build volume, an advanced class of materials known as Functionally Graded Materials (FGM) [1][6].

Although some authors argue that the production cost will drop as technology evolves, manufacturing metal components by AM is still only justifiable when a significant reduction in lead time, inventory cost, part weight or part count takes place [7]. Furthermore, the lack of diffuse knowledge of process dependent geometry limitations and output material properties, restrict the choice of manufacturing process according to the availability of material data still in the design phase [8].

In this context, the mechanical properties resulting from the process, are of special interest given the fact that metals are extensively used to withstand the mechanical loads of a variety of applications. Information extracted from stress-strain curves such as Young's modulus (E), elastic limit (Sy) and tensile strength (Su) are the baseline information for the mechanical design of structural components as illustrates Figure 2.

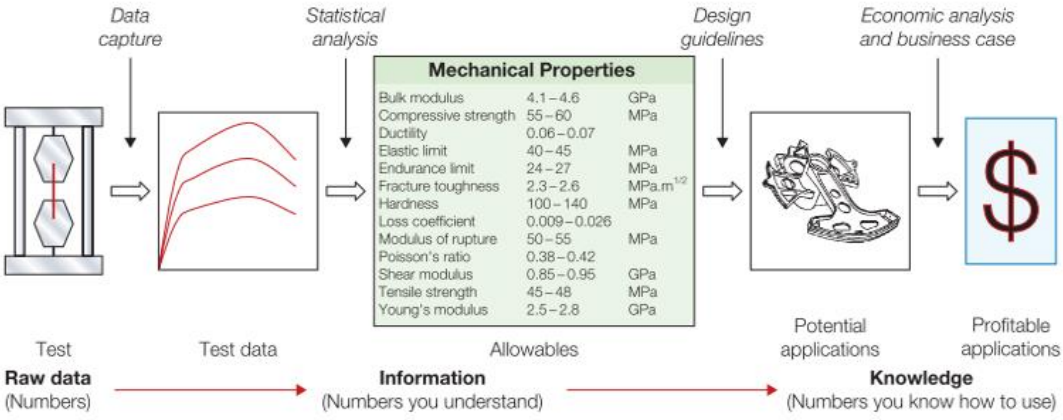

Figure 2 - Types of material information. Structured data for design "allowables" and the characteristics of a material that relate to its ability to be formed, joined, and finished; records of experience with its use; and design guidelines for its use [8].

Even though an enormous effort has been made for the last decade in order to standardize manufacturing practices and data reporting on mechanical properties, a collective understanding of the AM design paradigm as well as a database of material properties for different processing conditions is still required in order to democratize the technology [9][7].

1.1 GOALS

1.1.1 General goals

Considering the context described previously, the general goal of the present study is to propose a method to map the effects of key geometrical and processing parameters on the mechanical properties of samples produced by DED-LP. It is of the author's interest, that the study finds its use as input information for product development engineers interested on prototyping or manufacturing functional components using the technology.

1.1.2 Specific goals

In order to reach the general goal, the specific goals of the study are:

1. Select from the literature, critical geometric features that can induce variation in mechanical properties (e.g. aspect ratio, wall thickness, curvature radius and part height).
2. Select from the literature, critical processing parameters (e.g. processing speed, laser power and overlap distance) that can induce mechanical property variation;
3. Define processing parameter levels that result in a stable process for manufacturing the selected geometric features;
4. Successfully manufacture geometries with selected features and machine local samples for uniaxial tensile tests;
5. Conduct mechanical tests to characterize:
    a. Elastic modulus (E);
    b. Elastic limit (Se);
    c. Tensile strength (Su);
    d. Elongation at fracture (ε);
6. Report the dependency of the measured values on the build direction and other geometric and process parameters;

2 LIRETATURE REVIEW

2.1 ADDITIVE MANUFACTURING

Additive manufacturing (AM) can be defined as a process of joining materials to make parts from 3D model data, usually layer upon layer, as opposed to subtractive manufacturing and formative manufacturing methodologies [10].

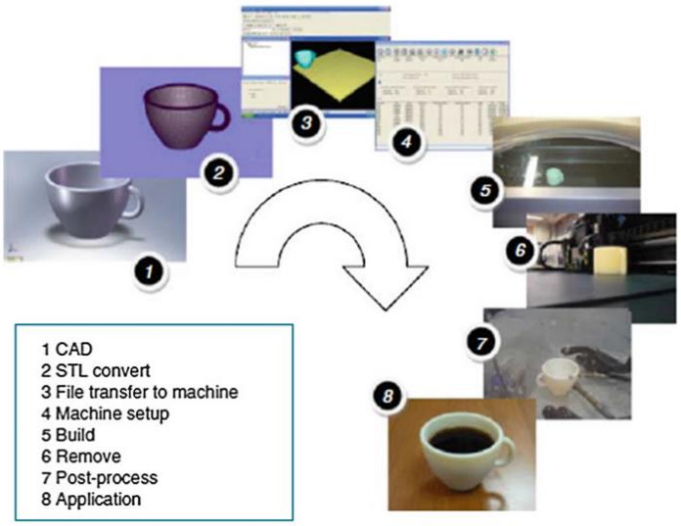

Figure 3 - Generic process of CAD to part, showing eight stages [11].

The idea was first documented in 1892 when Blanther applied the technique for building molds for topographic maps in three dimensions, but now it has developed into a highly digital manufacturing process, usually following the steps illustrated in Figure 3 to convert a digital 3D geometry into a physical part. The starting point is a 3D CAD model that is virtually sliced into thin layers with layer thickness of 20 µm – 1 mm, depending on the AM process. Based on this data the physical part is then built by repetitive deposition of single layers, locally melting the material by a heat source [4]. The part is then removed and usually post-processed before being ready for the application.

AM methods can essentially be classified by the nature and aggregate state of the feedstock as well as by the binding mechanism between the joined layers of the material [4]. A list of process categories is available in Table 1, highlighting the suitability of each category to produce dense metal parts.

Table 1 - Categories of additive manufacturing and suitability for producing dense metal parts. Adapted from [10], [12], [13].

Category	Example	Processed materials	Density of metal parts
Binder Jetting	3D printing;	Metals, Polymers, Composites, Ceramics	Low
Directed Energy Deposition	WAAM[1], Laser Cladding;	Metals	High
Material Extrusion	FDM[2]	Thermoplastics, Waxes	-
Material Jetting	Polyjet	UV curable resins	-
Powder Bed Fusion	SLS[3], SLM[4]	Metals, Thermoplastics, Ceramic	High
Sheet Lamination	Sheet forming	Metals, Polymers, Paper	High
Vat Polymerization	Stereolithography	UV curable resins, Wax, Ceramic	-

[1] Wire Arc Additive Manufacturing;
[2] Fused Deposition Modeling;
[3] Selective Laser Sintering;
[4] Selective Laser Melting;

AM has attracted much attention recently due to the potentials mentioned earlier in the introduction but in the present work, one of the processes suitable for processing metals (Directed Energy Deposition) will be discussed in further detail.

2.1.1 Directed Energy Deposition

Directed Energy Deposition, or DED, is defined as an additive manufacturing process in which focused thermal energy is used to fuse materials by melting as they are being deposited [14]. DED systems comprise multiple categories of machines using laser beam (LB), electron beam (EB), or arc plasma energy sources as summarized in Figure 4.

Feedstock material typically comprises either powder or wire. Deposition typically occurs either under inert gas (arc systems or laser) or in vacuum (EB systems) [14]. The process was a natural evolution of welding techniques and the first of its kind was LENS ®, documented in 1998 by the Sandia Labs in Albuquerque, New Mexico [1].

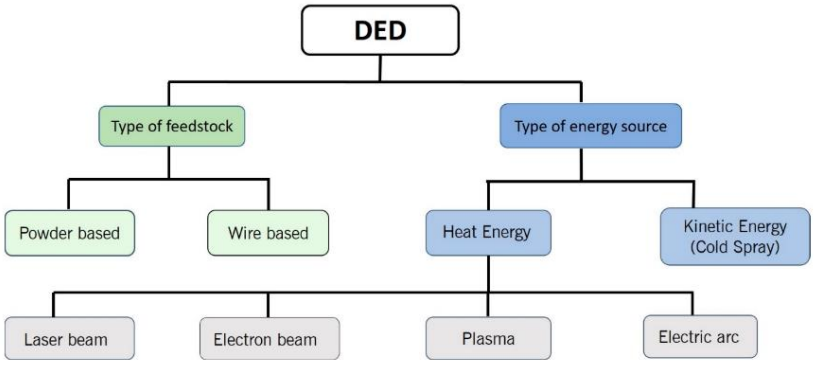

Figure 4 - Classification of Directed Energy Deposition (DED) systems [15].

A variety of names are currently used to refer to DED processes, some of which are proprietary as the precursor Laser Engineered Net Shaping or LENS® mentioned earlier. Other

frequently found in the literature are Wire Arc Additive Manufacturing or WAAM, Electron Beam Freeform Fabrication, Laser Metal Deposition and 3D Laser Cladding, describing processes of the same nature that differ in the types of energy source, feedstock material and atmosphere criticality.

A short introduction of laser technology will be given since in the present work we focus on a laser-based system with powder as feedstock. Further information can be found on F3187 standard guide for Directed Energy Deposition of Metals [14].

2.1.2 Laser technology

The term "laser" was originally an acronym for *Light Amplification by Stimulated Emission of Radiation*, characterizing a special process of light amplification, but is often used to represent a special source of light. Laser, as a special type of electromagnetic radiation, can be described by its wavelength (λ) and intensity (I), differing from general light in its high degrees of directionality, monochromaticity and coherence [16].

The history of laser began with an appropriate description of electromagnetic radiation formulated by Maxwell in 1873. The following discoveries included the processes of *spontaneous emission* and *absorption* and the process of *stimulated emission* postulated by Einstein in 1917. In 1960, Theodore Mainman reported about the pulsed laser activity of a ruby laser for the first time [17].

Table 2 - Some important commercial lasers. Adapted from [16].

Laser	**Wavelength**	**Average power range**
Carbon dioxide (CO_2)	10,6 µm	Milliwatts to tens of kilowatts
Nd:YAG	1,06 µm	Milliwatts to hundreds of watts
	532 nm	Milliwatts to watts
Nd:glass	1,05 µm	Watts
Diodes	Visible and IR	Milliwatts to kilowatts
Argon-ion	514,5 nm	Milliwatts to tens of watts
	448,0 nm	Milliwatts to watts
Fiber	IR	Watts to kilowatts
Excimer	Ultraviolet	Watts to hundreds of watts

Since 1960, different types of laser have been developed as listed in Table 2, greatly varying in terms of dimensions, output power and emission wavelength (λ) [17], the last characteristic being of special importance to understand the interaction between laser and matter.

According to Poprawe [18] the fundamental principles involved in laser material processes are related to the absorption of light by the workpiece and its partial conversion to heat. The absorption depends on the wavelength and polarization of the laser light, on the material physical properties and on the characteristics of the workpiece surface [18]. Figure 5 (a) illustrates absorption coefficients of different metals as a function of the wavelength of the incident radiation showing that certain laser sources are better absorbed by specific materials.

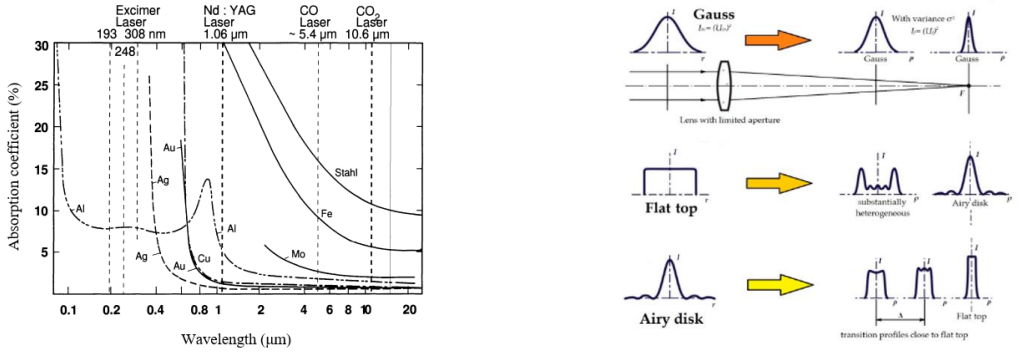

(a) (b)

Figure 5 – (a) Absorption coefficient of a variety of metals as function of the wavelength of the incident radiation [19]; (b) Example of focusing feature of disk laser beam and power density distribution at focal point [20].

The laser energy is not homogeneously distributed along a cross section of a laser beam as illustrates Figure 5 (b) and its distribution depends on the wavelength, beam quality and the focusing optics. From the irradiated surface, a heat front moves into the inner material by conduction due to the developed temperature gradients. The heat flux lead to rise in temperature, depending on the absorbed intensity, the duration of the interaction, the beam radius at the surface, the velocity of the workpiece relative to the laser beam and the thermo-physical parameters of the material like heat conductivity and heat capacity [18].

High energy intensities available at a small controllable area on the intersection between the laser beam and the workpiece surface, make the laser a well-suited tool for additive manufacturing processes. With the right combination of laser source and material, it is possible to melt and deposit metal on specific regions of a workpiece creating metallurgical bonds, layer by layer, until whole functional components are built.

2.2 DIRECTED ENERGY DEPOSITION LASER WITH POWDER (DED-LP)

In contrast to powder bed technologies, DED-LP technology provides a high build rate and allows for larger build volumes although presenting lower layer thickness resolution.

Depending on the main parameters, build rates up to 300 cm^3/h can be achieved using a layer thickness of 40 µm – 1 mm. Feed rates between 4 g/min and 30 g/min are realized for the deposition of metal powder [4].

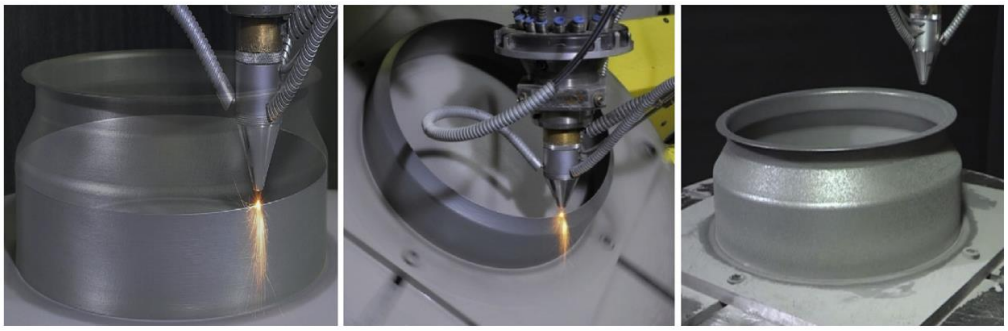

(a) (b) (c)

Figure 6 – IN718 helicopter engine combustion chamber fabricated by a five-axis laser DED process. (a) Deposition showing the 2.5-dimensional tool path; (b) Multiaxis deposition; (c) Finished part [3].

Moreover, as the material is melted while being deposited, it is possible to use 4 or 5-axis systems, as show Figure 6, to build structures with high overhang angles, reducing or eliminating the undesired metal support structures and reducing component postprocessing time [21]. One particular benefit of this characteristic is the potential to deposit material onto curved surfaces and existing metal structures. For this reason, one of the DED technologies, referred to as laser Cladding, is often used to repair damaged parts, particularly for the aerospace industry [5].

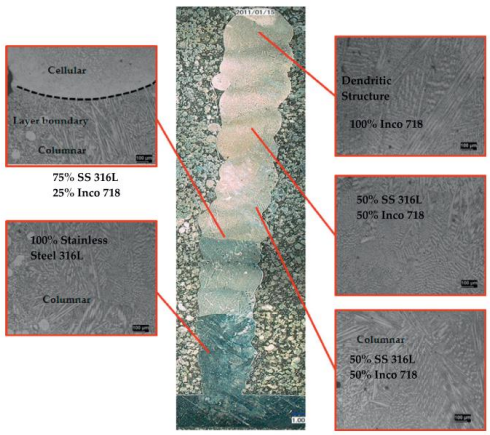

Figure 7 - Transverse cross section showing the transition between 100% 316L to 100% Inconel 718 from bottom to top [22].

Regarding the choice of feedstock material, one of the main advantages of using powder, is the capability of mixing different powders during the deposition, thus enabling the creation of gradient metal alloys in-situ, also known as functionally graded materials (FGM) as

illustrates Figure 7. The concept extends the design space to components that can be made of a continuum structure that uses cost-intensive alloys in highly-loaded regions, and cheaper compositions in non-critical areas [22].

In order to make use of the full potentials of DED-LP process, a list of challenges and unanswered questions need to be addressed. This list includes uncertainties about predicting the geometry, metallurgical integrity and mechanical properties of the formed components. These outputs highly depend on interactions between laser beam, powder stream and scanning speed, which will be briefly discussed in the next sessions.

2.2.1 Process description

A DED-LP system comprises five fundamental subcomponents: laser source, inert gas, powder feedstock feed mechanism, positioner and a computer control system. The process consists in the formation of a melt pool in the substrate through absorption and conversion of irradiated laser energy into heat. Simultaneously powder is fed into this pool and melts, subsequently solidifying to form a layer of deposited material as illustrated by Figure 8. A strong fusion bond between added material and substrate is achieved immediately [23].

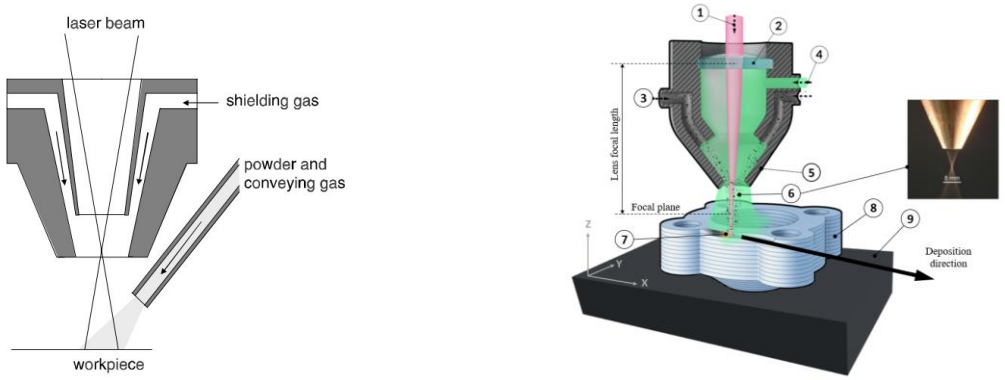

(a) (b)

Figure 8 – (a) Lateral powder supply [23]*; (b) Continuous coaxial powder nozzle during the deposition. (1) Process laser beam; (2) Focalizing lens; (3) Mix of metal powder with carrier gas; (4) Shielding inert gas; (5) Deposition nozzle; (6) Schematic (left) and realistic (right) views of a powder cone; (7) Melt pool; (8) Deposited structure; (9) Substrate. Adapted from* [24] *and* [18]*.*

A variety of nozzle configurations are reported in the literature, from lateral to coaxial, from discrete to continuous, two of which are schematically illustrated in Figure 8 (a) and (b). The powder is delivered to the melt pool by feeders, that can be based on various working principles, one of which consists of a container from which powder flows by gravity into a slot in a rotating

disk. The powder is transported to a suction unit from which it is transported by a gas stream to a powder nozzle. The volumetric powder feed rate is controlled by the dimensions of the slot and the speed of the disk [23].

The nozzle head is programmed to move along a path, previously defined by the user, and as it moves, continuously deposit material on the surface of the substrate, usually maintaining a constant distance between the nozzle tip and the surface. After forming the first layer, the nozzle moves in the positive Z direction, represented in Figure 8, and start adding material on top of the previously deposited layer. This process repeats until the entire part has been built. A schematic view of key input and output factors that affect the stability of the process are represented in Figure 8, some of which will be described in more detail later.

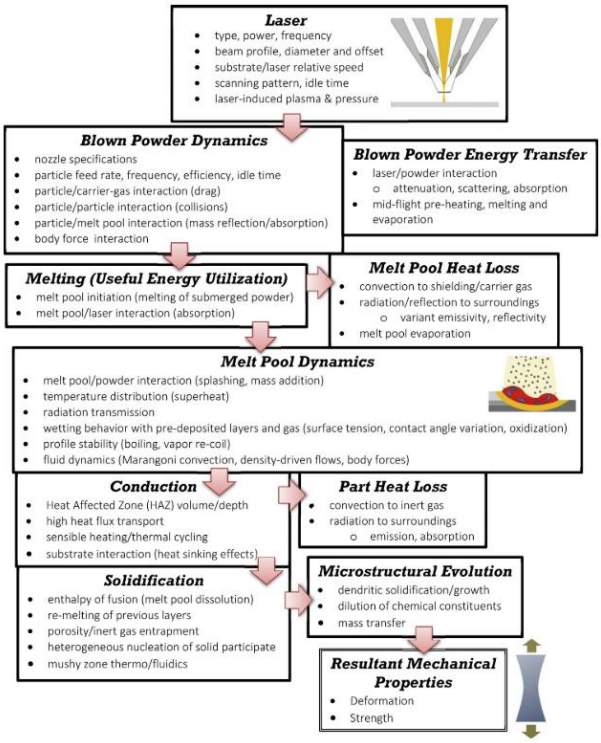

Figure 9 – Physical events occurring during DLD for given instant in time [25].

Along the process, several critical input variables schematically listed in Figure 9, interact with one another in a complex physical processes that involves light absorption, heat conduction and convection, mass diffusion and result in the geometry, microstructure, mechanical properties and other relevant characteristics [23]. The present study will focus on discussing geometric features, process parameters and their relationship with the resulting mechanical properties.

2.2.2 Thermal cycles and reported effects

During AM, a defined volume element, or voxel, of the material is usually subjected to a complex thermal cycle. This thermal cycle involves a rapid heating above melting temperature due to the absorption of the laser energy and its transformation into heat, a rapid solidification of the molten material after the heat source has moved on, and numerous re-heating and re-cooling processes when the following layers are welded and the voxel is still exposed to heat [8]. The effect is better pictured in Figure 10 (a) derived from a numerical investigation conducted by Manvatkar et. Al [26].

AM microstructure is therefore a result of the described thermal cycle. Independently of the material, a fine-grained structure has usually been observed for AM in comparison to other processes (e.g. casting) [4]. The effect can be explained by the high cooling rates of up to 12000 K/s as shown in Figure 10 (b) when compared with 1 – 100 K/s for casting [6], which itself is a result of the very local heat input and the small volumes of molten material [4].

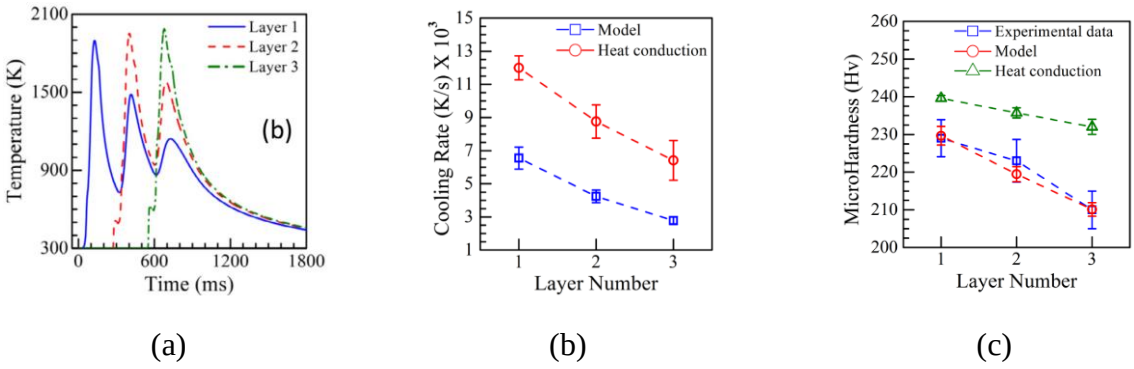

(a) (b) (c)

Figure 10 – (a) Simulated thermal cycles at three monitoring locations in the first three layers in a DED-L of 316 stainless steel at a laser power of 210 W and 12.7 mm/s speed; (b) Variation of cooling rate at three monitoring locations in the three layers. The results of the heat conduction calculations are from the literature; (c) Computed and the experimentally determined hardness values in three layers compared with heat conduction model; [26]

The temperature gradients are obviously influenced by several process parameters, e.g. the energy density, laser power, scanning speed, layer thickness and pre-heating temperature, if applied. Temperature gradients are also affected by the property gradients along the voxels of the structure. The presence of solidified materials on previous layers typically increase the heat conduction in the build direction compared with other special directions, what can explain the observed anisotropy in microstructure and mechanical properties [4].

For constant laser power and scanning velocity, the layer width and peak temperature increase while the cooling rate decreases toward the top layers as shown in Figure 10 (b) extracted from simulated results [26]. As a result, the solidified deposit usually exhibits finer grain structure close from the substrate with coarser grains towards the top. Correspondingly, the yield strength and hardness also reduce from the bottom toward the top layers [27]. Figure 10 (c) illustrates simulated values that match with experimental data.

2.2.3 Residual porosity and reported effects

As porosity facilitates crack propagation and deteriorates mechanical properties, the manufacture of parts with a high density, typically greater than 99.5%, is the first goal in AM process optimization [4]. Among other influences, part density depends on the applied volume energy

$$E_V = \frac{P_L}{v_S h_S D_S} \tag{1}$$

Where P_L is the laser power, v_S stands for the scan speed, h_S is the hatch distance and D_S the layer thickness of the deposited layer.

According to Herzog et. Al [4], too low energy input will result in unmolten material and thus reduced density by the formation of irregular-shaped voids. On the other hand, too high energy input will lead to higher melt pool dynamics and keyholing phenomenon resulting in spherical shaped pores formed due to entrapped gas, formed during evaporation of material, and reducing part density [4]. Figure 11 shows diagrams of the resulting pores geometry as well as a graph of the desired processing condition that generates minimum porosity.

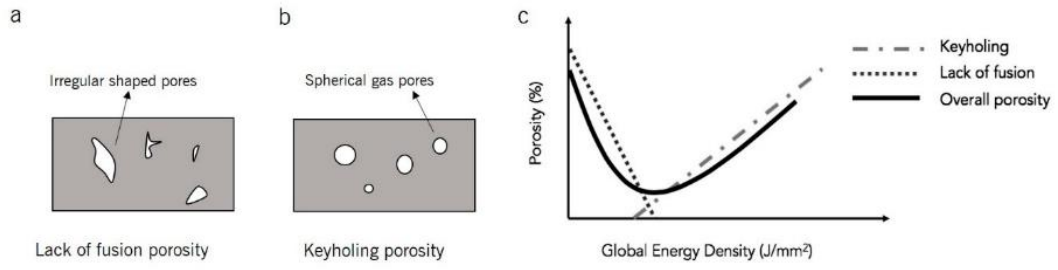

Figure 11 - Schematic showing: (a) Lack of fusion porosity (interlayer porosity), (b) keyholing porosity (intralayer porosity), and (c) the intersection of interlayer and intralayer porosity with respect volume energy [15].

According to Razavi et. Al [28][29] and Koike et. Al [30], the static strength of Ti-6Al-4V and Inconel 625 do not vary significantly between AM porous and non-porous specimens

compared with wrought specimens. On the other hand, the presence of stress raisers reduce the ductility of materials significantly and for this reason, fatigue strength of porous specimens reduce significantly as the presence of stress raisers facilitates fatigue crack initiation and fatigue crack propagation along the sample [29].

2.2.4 Reported strength and dependence on other factors

The resulting static mechanical properties of components manufactured by DED-LP have been documented for a variety of materials and processing conditions. Although the effects of processing parameters have been investigated to low cost materials such as iron [31], the ultimate tensile strength (UTS), yield strength (YS), elongation (ε) and elastic modulus (E) of tool steels, high speed steels, stainless steels and high-performance alloys such as Ti-6Al-4V and IN618 are more commonly discussed in the literature [32][33][34].

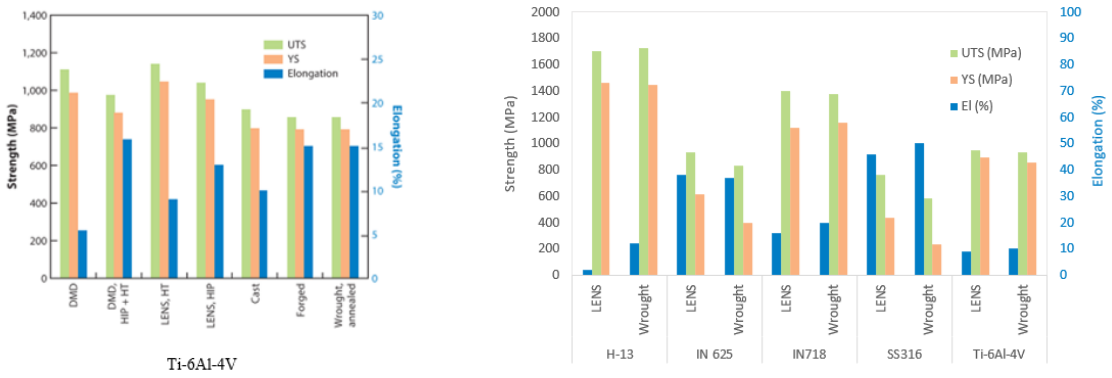

(a) (b)

Figure 12 – (a) Comparison of AM Ti-6Al-4V under different conditions with resulting properties of other manufacturing processes. Abbreviations: DMD, direct metal deposition; HT, heat treated; HIP, hot isostatic pressing; LENS, laser-engineered net shaping; UTS, ultimate tensile strength; YS, yield stress. Adapted from [32]. *(b) Comparison between mechanical properties of different metals manufactured by DED (LENS) and Wrought processes. Adapted from* [33].

Tensile strength and yield strength resulting from DED-LP processes (e.g. LENS, DMD) exhibit average values similar or higher to those resulting from casting and forging for different metals, manufacturing processes and treatments as illustrates Figure 12. Despite the average higher strength, DED-LP processed materials present lower elongation at fracture, what can be increased by appropriate heat treatment [32].

Griffith et. Al [33] reported variations in mechanical properties of H13 tool steel with respect to power and velocity settings. According to the study, higher heat input yielded lower ultimate tensile strength, higher yield strengths and higher elongation values. The author

attributes the results to the different melt pool sizes generated what have an impact on the cooling rates, with higher cooling rates resulting in higher strength and lower ductility.

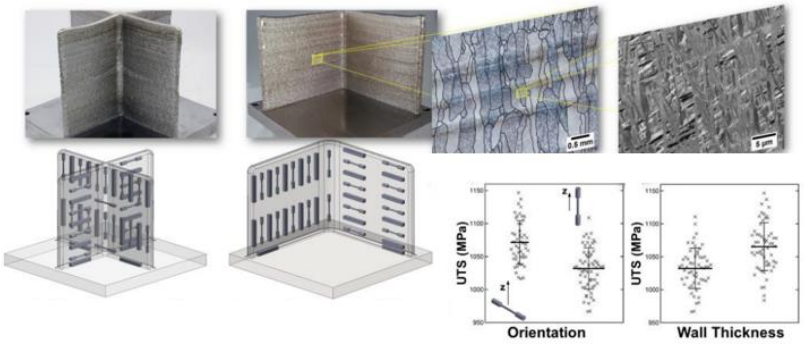

Figure 13 – Role of geometry on properties of AM Ti-Al-4V structures. Built structures, position and orientation of specimens within the part and resulting properties.

The dependency of mechanical properties and microstructure of Ti-6Al-4V on the geometry of the part and specimen orientation was investigated by Keist and Palmer [35], concluding that the orientation, wall thickness, part design and part height are significant factors that affect the static strength of the resulting structure. Higher ultimate tensile strength was measured for specimens: (1) with long dimension parallel to the substrate; (2) located on the bottom of the structure; (3) extracted from thicker walls, or (4) extracted from thin walls from L-Shaped structures. The results are summarized in Figure 13.

Although the effect of geometry on strength is noticeable, it is worth to mention that mechanical properties present similar behavior for conventional processes such as casting for instance, where the wall thickness impose different solidification regimens, resulting in different microstructures and mechanical properties [36].

3 MATERIALS AND METHODS

3.1 METHODOLOGY

The project will be split in four phases: (1) Material selection; (2) Geometry and processing conditions; (3) Production of samples; (4) Tensile tests and analysis. The phases are summarized in Figure 14 and further details are described below.

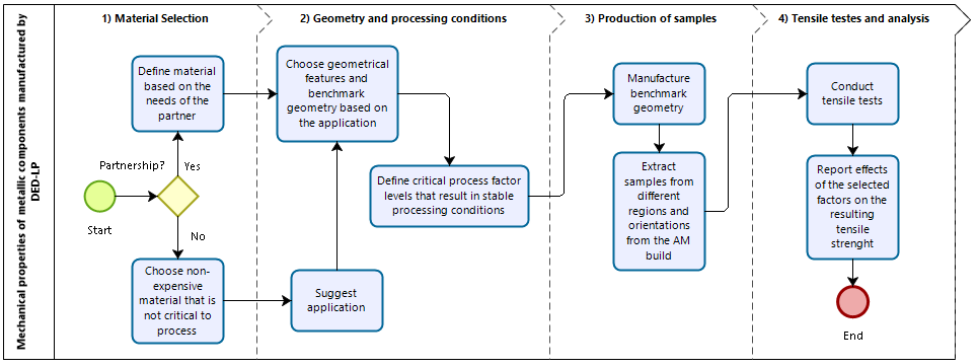

Figure 14 - Summary of project phases

The first stage of the project will be to select the appropriate metal composition for conducting the experiments, considering the range of applications, price and quality of raw materials available in the market. The decision might highly depend on possible partnerships with industry and if no partnership is stablished, the cost of the raw material will have a higher impact on the decision, with iron powder being the first option.

From that point, a benchmark geometry containing critical geometrical features will be developed or chosen from the literature considering the limitations of the available equipment and requirements of a given application (brought from a possible partner or suggested by the author based on literature review and past work experience). The next step will be to define critical factors and parameter levels that result in a stable process and dense metallic structures for the chosen material.

On the third stage, the benchmark geometry will be manufactured, and samples will be machined from inside the structure with appropriate geometry in accordance with recommendations from available standards. The last stage will be to conduct the tensile tests according to recommendations from the same standards, analyze and report the results, correlating the mechanical properties with selected factors.

3.2 TECHNICAL AND FINANCIAL RESOURCES

The benchmark geometry will be additively manufactured using the SL1 system, one of the laser systems available at the Precision Engineering Laboratory (LMP). The system is composed by a fiber laser model YLS-10000 from IPG Photonics, with wavelength of 1064nm and optic system with 300mm focal length delivering the beam with diameter 880 μm on the focal point. The system is also connected to a three-axis CNC machine, a disc powder feeder

system and gas lines which combined deliver up to 30g/min of powder with 20 l/min gas flow rate in a build volume of 300mm x 300mm x 300mm.

The tensile tests will be performed at LabMat using the MTS Criterion Model 45 with 10kN capacity. Powder characterization and microstructure analysis will be conducted using optical and scanning electron microscopy as needed. A summary of the main equipment resources that will be used is listed in Table 3. In a scenario of no partnership with industry, iron powder available at LMP will be selected as feedstock material and up to two cylinders of inert gas will be provided by the author.

Table 3 - List of equipment resources

Activity	Equipment	Laboratory
Optical microscopy	Leica ® DM 4000 MLED	LabMat
Scanning electron microscopy	Hitachi ® Tabletop Microscope	LMP
Production of samples	Laser source	LMP
Production of samples	Powder feeder	LMP
Production of samples	CNC	LMP
Tensile test	MTS Criterion Model 45	LabMat

2. SCHEDULE

The main planned activities are chronologically listed in Figure 15.

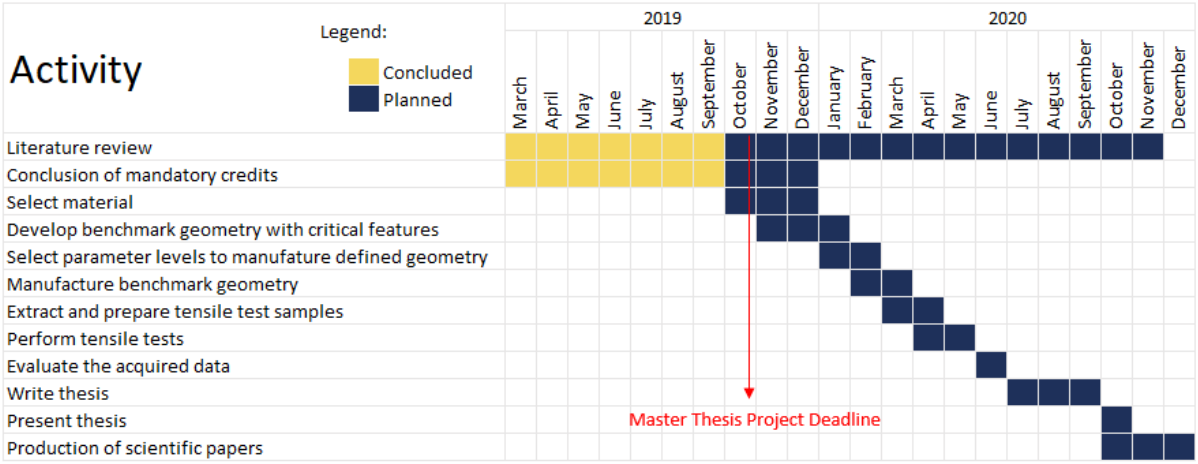

Figure 15 – List of planned activities and preliminary deliver dates

4 REFERENCES

[1] N. Volpato *et al.*, *Manufatura Aditiva - Tecnologias e aplicações da impressão 3D*. Blucher, 2017.

[2] P. Zhang, J. Liu, and A. C. To, "Role of anisotropic properties on topology optimization of additive manufactured load bearing structures," *Scr. Mater.*, 2017.

[3] R. Liu, Z. Wang, T. Sparks, F. Liou, and J. Newkirk, *Aerospace applications of laser additive manufacturing*. Elsevier Ltd, 2016.

[4] D. Herzog, V. Seyda, E. Wycisk, and C. Emmelmann, "Additive manufacturing of metals," *Acta Mater.*, vol. 117, pp. 371–392, 2016.

[5] A. Saboori, A. Aversa, G. Marchese, S. Biamino, M. Lombardi, and P. Fino, "Application of Directed Energy Deposition-Based Additive Manufacturing in Repair," *Appl. Sci.*, vol. 9, no. 16, p. 3316, 2019.

[6] T. DebRoy *et al.*, "Additive manufacturing of metallic components – Process, structure and properties," *Prog. Mater. Sci.*, vol. 92, pp. 112–224, 2017.

[7] D. L. Bourell, M. C. . Leu, and D. W. Rosen, "Roadmap for Additive Manufacturing: Identifying the Future of Freeform Processing," 2009.

[8] M. Ashby, *Materials selection in mechanical design: Fourth edition*, vol. 9780080952. 2011.

[9] D. L. Bourell, D. W. Rosen, and M. C. Leu, "The roadmap for additive manufacturing and its impact," *3D Print. Addit. Manuf.*, vol. 1, no. 1, pp. 6–9, 2014.

[10] ISO and ASTM, "ISO/ASTM 52900:2015(E) - Standard Terminology for Additive Manufacturing – General Principles – Terminology," vol. i, pp. 1–9, 2019.

[11] I. Gibson, D. Rosen, and B. Stucker, *Additive manufacturing technologies: 3D printing, rapid prototyping, and direct digital manufacturing, second edition*. 2015.

[12] C.-J. Bae, A. B. Diggs, and A. Ramachandran, *Quantification and certification of additive manufacturing materials and processes*. Elsevier Inc., 2018.

[13] T. Caffrey and T. Wohlers, "Additive manufacturing state of the industry," *Manuf. Eng.*, 2015.

[14] ASTM and ISO, "F3187 − 16: Standard Guide for Directed Energy Deposition of Metals 1," pp. 1–22, 2019.

[15] A. Dass and A. Moridi, "State of the Art in Directed Energy Deposition: From Additive Manufacturing to Materials Design," *Coatings*, 2019.

[16] C. B. Hitz, J. Ewing, and J. Hecht, *Introduction to Laser Technology*. 2012.

[17] R. Poprawe, K. Boucke, and D. Hoffman, *Tailored Light 1*. 2018.

[18] R. Poprawe, *Tailored Light 2 Laser Application Technology*. 2016.

[19] G. Herziger and H. Weber, *Laser in Technik und Forschung*. 1998.

[20] Y. Kawahito *et al.*, "Elucidation of the effect of welding speed on melt flows in high-brightness and high-power laser welding of stainless steel on basis of three-dimensional X-ray transmission in situ observation," *Weld. Int.*, vol. 31, no. 3, pp. 206–213, 2016.

[21] J. Xu, X. Gu, D. Ding, Z. Pan, and K. Chen, "A review of slicing methods for directed energy deposition based additive manufacturing," *Rapid Prototyp. J.*, vol. 24, no. 6, pp. 1012–1025, 2018.

[22] K. Shah, A. Khan, S. Ali, M. Khan, and A. J. Pinkerton, “Parametric study of development of Inconel-steel functionally graded materials by laser direct metal deposition,” *Mater. Des.*, vol. 54, pp. 531–538, 2014.

[23] M. Schneider, “Laser clading with powder effect of some machining parameters on clad properties,” 1998.

[24] Manufacturing Guide, “Laser Cladding 3D, LC3D | Find suppliers, processes & material.” [Online]. Available: https://www.manufacturingguide.com/en/laser-engineered-net-shaping-lens-0. [Accessed: 04-Jul-2019].

[25] S. M. Thompson, L. Bian, N. Shamsaei, and A. Yadollahi, “An overview of Direct Laser Deposition for additive manufacturing; Part I: Transport phenomena, modeling and diagnostics,” *Addit. Manuf.*, vol. 8, pp. 36–62, 2015.

[26] V. Manvatkar, A. De, and T. Debroy, “Heat transfer and material flow during laser assisted multi-layer additive manufacturing,” *J. Appl. Phys.*, vol. 116, no. 12, 2014.

[27] V. D. Manvatkar, A. A. Gokhale, G. Jagan Reddy, A. Venkataramana, and A. De, “Estimation of melt pool dimensions, thermal cycle, and hardness distribution in the laser-engineered net shaping process of austenitic stainless steel,” *Metall. Mater. Trans. A Phys. Metall. Mater. Sci.*, vol. 42, no. 13, pp. 4080–4087, 2011.

[28] S. M. J. Razavi, G. G. Bordonaro, P. Ferro, J. Torgersen, and F. Berto, “Porosity effect on tensile behavior of Ti-6Al-4V specimens produced by laser engineered net shaping technology,” *Proc. Inst. Mech. Eng. Part C J. Mech. Eng. Sci.*, vol. 0, no. 1, pp. 1–8, 2018.

[29] S. M. J. Razavi, G. G. Bordonaro, P. Ferro, J. Torgersen, and F. Berto, “Fatigue behavior of porous Ti-6Al-4V made by laser-engineered net shaping,” *Materials (Basel).*, vol. 11, no. 2, 2018.

[30] R. Koike, Y. Kakinuma, T. Aoyama, D. M. G. M. Co, and Y. Oda, “Study on correlation internal void and strength in direct energy deposition,” pp. 1033–1034, 2017.

[31] M. Ansari, A. Mohamadizadeh, Y. Huang, V. Paserin, and E. Toyserkani, “Laser directed energy deposition of water-atomized iron powder: Process optimization and microstructure of single-tracks,” *Opt. Laser Technol.*, vol. 112, pp. 485–493, 2019.

[32] J. J. Lewandowski and M. Seifi, “Metal Additive Manufacturing: A Review of Mechanical Properties,” vol. 46, no. 1, pp. 151–186, 2016.

[33] M. L. Griffith *et al.*, “Understanding the Microstructure and Properties of Components Fabricated By Laser Engineered Net Shapgin (LENS),” vol. 625, pp. 9–20, 2000.

[34] Y. Kok *et al.*, “Anisotropy and heterogeneity of microstructure and mechanical properties in metal additive manufacturing: A critical review,” *Mater. Des.*, 2017.

[35] J. S. Keist and T. A. Palmer, “Role of geometry on properties of additively manufactured Ti-6Al-4V structures fabricated using laser based directed energy deposition,” *Mater. Des.*, vol. 106, pp. 482–494, 2016.

[36] A. Handbook, “ASM Metals HandBook Volume 1 - Properties and Selections - Irons Steels and High and Performance,” *Technology*, vol. 2, p. 3470, 1990.